Design and Characterization of Asparagine- and Lysine-Containing Alanine-Based Helical Peptides That Bind Selectively to A·T Base Pairs of Oligonucleotides Immobilized on a 27 MHz Quartz Crystal Microbalance†

Hisao Matsuno, Kenichi Niikura, and Yoshio Okahata*

Department of Biomolecular Engineering, Tokyo Institute of Technology, Nagatsuta, Midori-ku, Yokohama 226-8501, Japan

Received July 21, 2000; Revised Manuscript Received November 9, 2000

ABSTRACT: We have systematically designed and synthesized six kinds of 16−17 mer alanine-based peptides containing four to six lysine (K) and one to four asparagine (N) residues to achieve the selective binding to A·T base pairs of DNA duplexes. The position and number of K and N residues were changed in the helical structure according to common features of the DNA-binding proteins, in which K and N residues are expected to interact electrostatically with phosphate groups and to interact with A·T base pairs by hydrogen bonding, respectively. The time courses of binding of these peptides to dA_{30}·dT_{30} and dG_{30}·dC_{30} duplexes immobilized on a 27 MHz quartz crystal microbalance (QCM) were studied in 10 mM phosphate buffer (pH 7.5) and 40 mM NaCl at 10 °C. The maximum binding amounts (Δm_{max}) on a nanogram scale and binding constants (K_a) could be obtained from the frequency decrease (mass increase) of the oligonucleotide-immobilized QCM. The conformation changes of the peptides upon binding to DNAs were monitored by circular dichroism (CD) spectroscopy. The four properly arranged N residues in the six-cationic K peptide, K6N4(d), resulted in a 5-fold higher affinity for A·T base pairs ($K_a = 5.9 \times 10^5\ M^{-1}$) than for G·C base pairs ($K_a = 1.2 \times 10^5\ M^{-1}$), and α-helices were clearly promoted by the binding to A·T base pairs from CD spectral changes.

According to X-ray crystallographic studies of DNA−protein complexes, the sequence specific DNA-binding proteins such as transcription factors have some similar DNA-binding domains (*1*−*4*). Many of these are classified as helix−turn−helix (*1*), Zn-finger (*2*), basic-region helix−loop−helix (*3*), and basic-region leucine-zipper (*4*) domains. These DNA-binding motifs have a common DNA recognition helix, in which cationic lysine (K) or arginine (R) residues at one side of the helix interact with a major groove of DNA strands, and hydrogen-bonding residues such as asparagine (N), glutamine (Q), and serine (S) at the same site are involved in the selective recognition of base pairs (see Figure 1A). The size and shape of an α-helix (cylindrical radius of 4−6 Å) is complementary to a major groove of B-form DNA (cylindrical radius of 6 Å), where the base pairs differ in hydrogen bond donor or acceptor patterns and hydrophobicity. Similar sequences were found for these α-helices by statistical analyses of DNA-binding proteins. These helices bind four or six base pairs of DNA through nonspecific electrostatic interaction between K or R residues and phosphate oxygen. As one of the hydrogen-bonding amino acids, N residues were well observed at a diagonal area, especially in position 1, in Figure 1A (*5*). The N residue has a terminal amide group that can make a matching hydrogen bond with A·T base pairs (Figure 1B) (*6*).

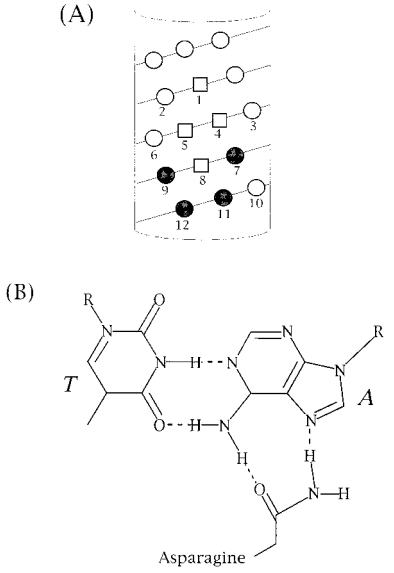

FIGURE 1: (A) Cylindrical structure of common features of the DNA recognition helix (see ref *5a*). (□) Hydrogen bonding amino acids such as N, Q, and S and (●) cationic amino acids such as K and R. The basic region of the GCN4-bZIP peptide has the following sequence ($N_1T_2E_3A_4A_5R_6R_7S_8R_9A_{10}R_{11}K_{12}$). **(**B**)** Specific hydrogen bonding between asparagine and an A·T base pair (see ref *6*).

Our goal is to design a simple α-helical peptide that exhibits sequence-specific DNA binding properties as a model of DNA-binding proteins. In the previous report (*7*), we have prepared six kinds of alanine-based α-helical peptides having only four to six cationic K residues, K4(a)−

† H.M. and K.N. thank the Japanese Society for the Promotion of Science for a fellowship.

* Corresponding author. Fax: +81-45-924-5836. E-mail: yokahata@bio.titech.ac.jp.

10.1021/bi001699o CCC: $20.00
Published on Web 03/01/2001

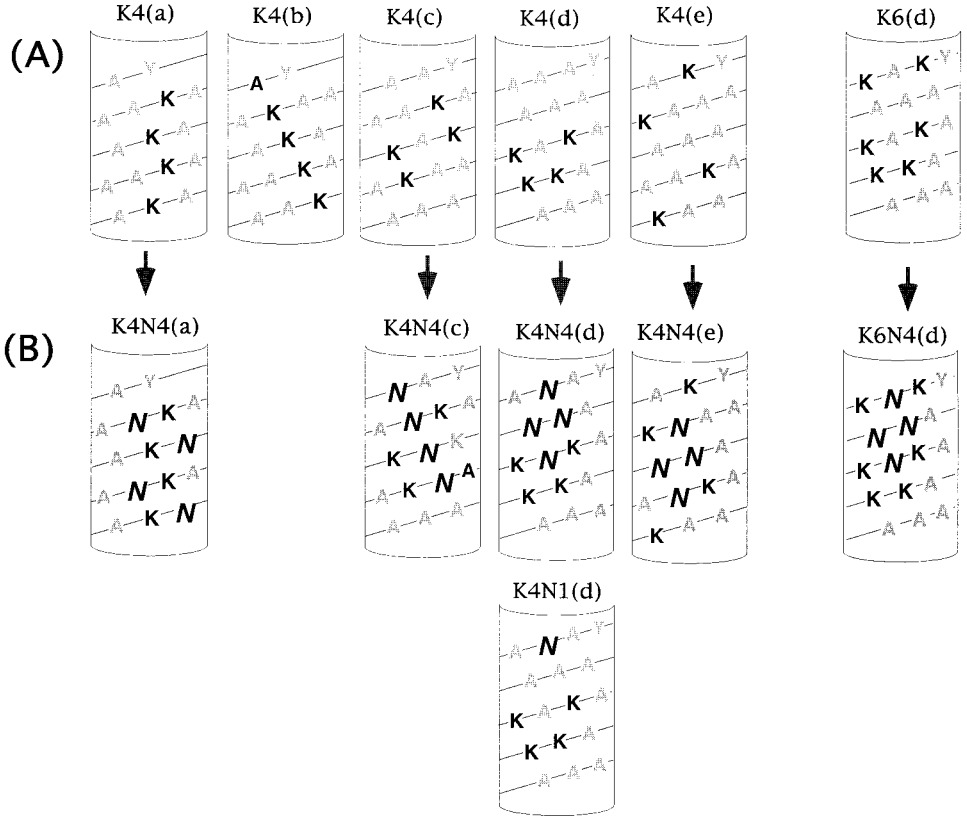

FIGURE 2: Cylindrical structures of (A) only cationic lysine (K)-containing alanine-based peptides and (B) both N- and K-containing peptides (16−17 mer). Tyrosine (Y) was introduced at the N terminus for easy detection by UV absorption, and the N and C termini were acetylated and amidated, respectively.

K4(e)[1] and K6(d) shown in Figure 2A. These peptides proved to bind selectively to a DNA duplex, but not a single DNA strand. However, these K4 and K6 peptides had no sequence specificity for DNA strands. Amphiphilic α-helical peptides have also been reported to bind selectively to DNA strands (*8*−*10*).

In this paper, focusing on sequence specificity and higher affinity for DNA strands, we designed six kinds of alanine-based α-helical peptides having hydrogen-bonding N residues as well as cationic K residues. The sequences are listed in Figure 2B as cylindrical forms. K4N4(a), K4N4(c), K4N4-(d), K4N4(e), and K6N4(d) have four N residues in addition to the K-containing peptides, K4(a), K4(c), K4(d), K4(e), and K6(d), respectively. K4N1(d) has one N residue in addition to the K4(d) peptide. We expected the sequence selectivity for A·T base pairs due to hydrogen bonding between the amide group of N residues and an A·T base pair (*6*).

The binding of proteins or peptides to DNA strands has been conventionally studied by a gel mobility shift assay (*11*). This technique is widely used in molecular biology; however, it is still difficult to detect the binding of small oligopeptides to small oligonucleotides and to evaluate quantitatively the binding process and amount. To provide general rules about how helical peptides bind to the major groove of DNA strands, systematic and quantitative methods are required. We have introduced a quartz crystal microbalance (QCM) technique to detect molecular recognition between biomolecules (*7*, *12*), and its resonance frequency decreases linearly with an increase in the mass on the QCM electrode at the nanogram level (*13*, *14*). Oligonucleotides such as dA_{30}·dT_{30} or dG_{30}·dC_{30} were immobilized on a QCM, and the frequency decreased (mass increased) in response to the binding of peptides to the oligonucleotides on the QCM plate. The 27 MHz QCM used in this study has a sensitivity of 0.6 ng cm^{-2} of mass change per hertz of frequency decrease (*12a*), the binding of 16−17 mer oligopeptides to be assessed. The maximum binding amount (Δm_{max}) and binding constants (K_a) of all peptides for both a dA_{30}·dT_{30} or a dG_{30}·dC_{30} duplex were obtained. These K_a values were compared with those obtained with CD spectral changes, which showed the α-helix content increased from a random coil due to the neutralization of positive K groups in the peptides (*9b*, *15*). We found that the peptides having N residues at the proper positions, such as K6N4(d), exhibited higher affinities for a dA_{30}·dT_{30} duplex [$K_a = 5.9 \times 10^5$ M^{-1}, for K6N4(d)] than for a dG_{30}·dC_{30} duplex [$K_a = 1.2 \times 10^5$ M^{-1}, for K6N4(d)], in which two or three helix peptides bound per strand.

EXPERIMENTAL PROCEDURES

Materials. Single-stranded oligonucleotides such as dT_{30} or dC_{30} and biotinylated dA_{30} or biotinylated dG_{30} were

[1] Abbreviations: QCM, quartz crystal microbalance; Δm_{max}, maximum binding amount; K_a, binding constant; CD, circular dichroism; bZIP, basic region leucine-zipper; K4(a), YAAKAAAKAAKAAAKA; K4(b), YAAAKAAKAAKAAKAA; K4(c), YAAAKAAKAKAA-KAAAA; K4(d), YAAAAAAKAKAKKAAA; K4(e), YKAAAA-KAAAAKAAAAK; K6(d), YKAKAAAAKAKAKKAAA; K4N4(a), YAAKNANKAAKNANKA; K4N4(c), YANAKNAKNKANKAAAA; K4N4(d), YANAANNAKNKAKKAAA; K4N1(d), YANAAAAAKA-KAKKAAA; K4N4(e), YKAAANKANNAKNAAAK; K6N4(d), YKN-KANNAKNKAKKAAA.

ordered from Pharmacia, Co. Oligonucleotides were purified by reversed-phase HPLC, and their concentrations were determined by an optical density measurement taken at 260 nm.

Peptides were prepared from a single stepwise manual solid-phase peptide synthesis using Fmoc (9-fluorenylmethoxycarbonyl) amino acids: Fmoc-Ala-OH, Fmoc-Asn-OH, Fmoc-Lys(Boc)-OH, and Fmoc-Tyr(tBu)-OH (*7*). The coupling reaction was performed with 250 mg of Fmoc-NH-SAL resin (0.13 mmol) and Fmoc amino acid (0.4 mmol) in the presence of BOP (0.4 mmol), *N*,*N*-diisopropylethylamine (DIEA) (1.2 mmol), and 1-hydroxybenzotriazole (0.5 mmol) in *N*-methylpyrolidone (NMP) for 40 min. Completion of the coupling was monitored by Kaiser test, and the coupling reaction was repeated until it reached completion. Removal of the Fmoc group was performed by treatment with a 20% piperidine/NMP mixture. The amino termini were acetylated with anhydrous acetic acid, and the peptides were cleaved from the resin with a cleavage mixture containing thioanisole (1.2 mL), 1,2-ethanedithiol (0.6 mL), and *m*-cresol (0.2 mL) in trifluoroacetic acid (7.48 mL), and then desalted by Sephadex G-10 chromatography in 5% acetic acid. Purification was carried out by reversed-phase HPLC with a Cosmosil 5C18AR-II column (Nacarai Tesque, 10 mm × 250 mm) and a linear gradient of acetonitrile and water with 0.1% trifluoroacetic acid (1 to 60% acetonitrile over the course of 30 min, at a flow rate of 3 mL/min). Each peptide was identified by matrix-assisted laser desorption ionization (MALDI) TOF-mass spectrometry. Other chemicals were purchased from Tokyo Kasei, Co., and Sigma Co. and used without further purification.

A 27 MHz QCM and Calibration. A 27 MHz, AT-cut QCM is commercially available from Showa Crystals Co. (Chiba, Japan). The diameter of its quartz plate is 8 mm, and Au electrodes are deposited on both sides (2.5 mm diameter, 4.9 mm^2 area). The one side of the quartz crystal was sealed with a rubber casing and kept in an air environment to avoid contact with the ionic aqueous solution, while the other is exposed to aqueous buffer solution (*12*, *14*). The QCM measurement equipment was described in previous papers (*7*, *16b*). Calibration of the 27 MHz QCM was also described in previous papers in that a frequency decrease of 1 Hz corresponded to a mass increase of 0.62 ± 0.1 ng cm^{-2} on the QCM electrode (*7*, *9*, *12*, *16b*). The noise level of the 27 MHz QCM was ±2 Hz in buffer solution at 20 °C, and the standard deviation of the frequency was ±5 Hz for 12 h in buffer solution at 20 °C.

Immobilization of DNA on a 27 MHz QCM. Immobilization of a biotinylated dA_{30}·dT_{30} duplex or biotinylated dG_{30}·dC_{30} duplex to an avidin-bound QCM has been reported previously (see Figure 3) (*7*, *16*). To the cleaned bare Au electrode side of the QCM plate was immobilized 3,3′-dithiodipropionic acid, and then carboxylic acids were activated as *N*-hydroxysuccinimide esters on the surface. The activated carboxyl groups were reacted with surface amino groups of avidin (MW = 68 000). The frequency decrease reached equilibrium at 800−1000 Hz (480−600 ng cm^{-2}) for 1 h. Avidin (80 nm^2 section area) was confirmed from frequency changes of 800−1000 Hz (480−600 ng cm^{-2}) to bind as a monolayer on the electrode (25−30 ng on 4.9 mm^2). Avidin was not removed from the electrode by rinsing it with an aqueous solution several times. The QCM was immersed in the aqueous solution of ethanolamine to deactivate the carboxyl group as β-hydroxyethylamide.

The avidin-bound QCM was immersed in the aqueous buffer solution (pH 7.9, 10 mM Tris-HCl, 0.2 M NaCl) of the biotinylated dA_{30}·dT_{30} or dG_{30}·dC_{30} duplex at 25 °C. After 30 min, when the frequency decreased ∼200 ± 5 Hz (mass increase of 120 ± 3 ng cm^{-2}) in about 30 min, the QCM was picked up to control the immobilization amount. The biotinylated dA_{30}·dT_{30} strand is calculated to cover ∼15% of the Au electrode and to bind to one of four binding sites of an avidin molecule.

Binding of Peptides to DNA Strands on a QCM. A dA_{30}·dT_{30}- or dG_{30}·dC_{30}-immobilized QCM was soaked in 8 mL of aqueous solution (10 °C, pH 7.5, 10 mM phosphate, 40 mM NaCl), and the resonance frequency of the QCM was defined as zero position after equilibrium. The stability and drift of the 27 MHz QCM frequency in the solution were ±5 Hz for 12 h at 10 °C. The frequency change of the QCM in response to the addition of 10−100 μL of an aqueous solution of peptides was recorded with time. The solution was stirred to avoid any effect of diffusion of peptides, and the stirring did not affect the stability or the amount of frequency changes.

Circular Dichroism (CD) Spectra. Spectra were observed with a J-720WI spectropolarimeter (Nippon Bunkou, Co., Tokyo, Japan) using a quartz cell (2 mm cell length, 10 °C, pH 7.5, 10 mM phosphate, 20 mM NaCl). At first, the CD spectrum of DNA only was observed, and after incubation of DNA with the peptide for 10 min, the spectrum of the peptide−DNA duplex was observed. The CD differential spectrum of the peptide was obtained by subtracting the DNA spectrum from the peptide−DNA spectrum.

RESULTS

Immobilization of DNA Strands on a QCM. An immobilization figure of dA_{30}·dT_{30} or dG_{30}·dC_{30} strands is shown in Figure 3, according to our previous paper (*7*, *16*). At first, avidin molecules were covalently bound on carboxyl groups on the one side of Au electrodes (4.9 mm^2) of a 27 MHz QCM, in which the other side of Au electrodes was sealed with a rubber casing to avoid contact with the buffer solution (see Experimental Procedures) (*7*, *12*, *16*). The presence of a monolayer of avidin molecules on the surface of the electrode was confirmed by the frequency decrease (mass increase) of the QCM (480−600 ng cm^{-2}, 7 × 10^{-12} mol cm^{-2}).

Biotinylated dA_{30} hybridized with dT_{30} was immobilized on the covalently bonded avidin layer on the QCM surface by immersing the QCM for ∼30 min in the aqueous buffer solution of DNAs (120 ± 3 ng cm^{-2}, ∼6 × 10^{-12} mol cm^{-2}). The biotinylated dA_{30}·dT_{30} strand (3.2 nm^2 area per molecule) can be calculated to cover ∼15% of the Au electrode (4.9 mm^2 area), and to bind to one of four binding sites of an avidin molecule. The immobilized amount of DNA strands on the QCM was controlled to be ∼15% coverage to allow enough space for oligopeptide binding. The immobilized amount of DNA strands on the QCM could be controlled from 10 to 80% by the immersion time. The dG_{30}·dC_{30} strands could also be immobilized on a QCM in the same amount in the same manner.

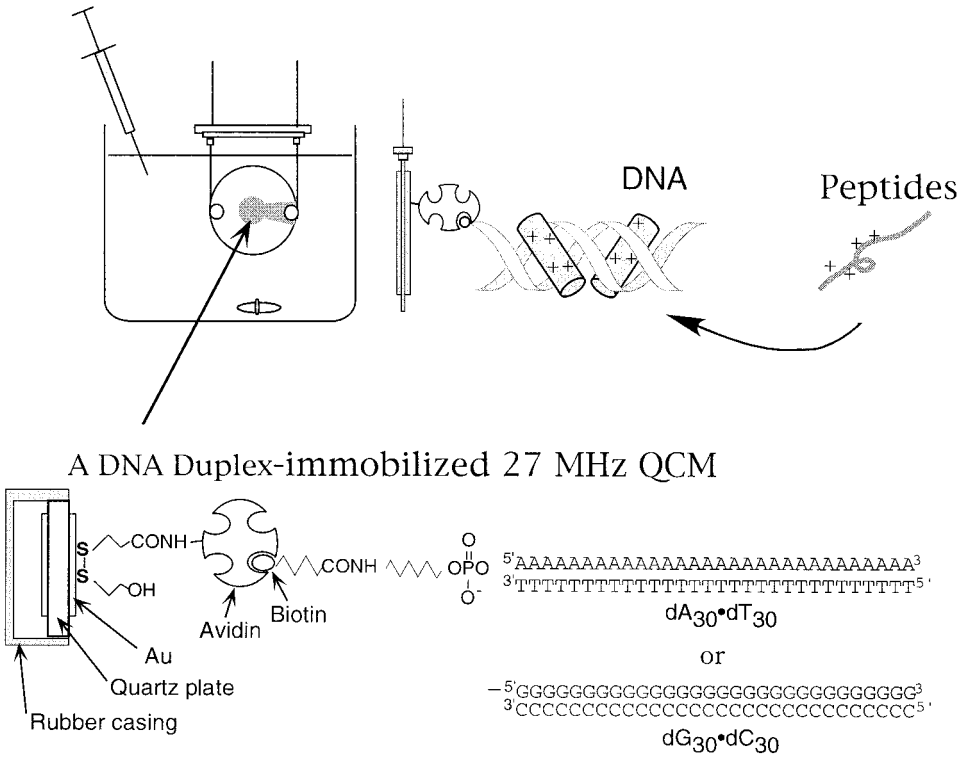

FIGURE 3: Schematic illustration of a 27 MHz QCM measurement system and chemical structures of immobilized DNA strands on the Au electrode (4.9 mm^2 area) on the QCM.

Design Criteria of Peptides. As shown in Figure 2A, we have designed five new K4 peptides in which the four basic K residues exist at different positions in cylindrical forms and one K6(d) with two additional K residues (*7*). Also, we have synthesized six peptides having one to four N residues in addition to the lysine residues of K4(a)−K4(d) and K6(d). K4N4(a) has four N residues along the perpendicularly arranged K4 groups of K4(a). K4N4(c) has four N residues in the middle of two lines of K4 groups. K4N4(d) and K4N1(d) were designed to imitate the naturally occurring DNA-binding proteins shown in Figure 1A. Since position 1 in Figure 1A was often occupied by an N residue, we designed the K4N1(d) peptide having one N residue for the v-shaped K4 groups. K4N4(e) has four N residues diagonally arranged within randomly arranged K4 groups. K6(d) has two more K residues than K4(d), which provided the highest affinity for a dA_{30}·dT_{30} duplex (1.1×10^5 M^{-1}). K6N4(d) has four N residues diagonally arranged in addition to the v-shaped K6 groups, mimicking the cationic position of the bZIP peptide, one of the typical DNA-binding motifs (*17*).

Time Course of the Peptide Binding to DNAs. The DNA-immobilized QCM was soaked in 10 mM phosphate buffer (pH 7.5) and 40 mM NaCl at 10 °C. After the frequency became stable (within ±1 Hz), an aliquot of the aqueous solution of the peptide was added to the aqueous solution. Figure 4A shows typical time courses of the frequency decrease (mass increase) of a dA_{30}·dT_{30} or dG_{30}·dC_{30} strand-immobilized QCM, responding to the addition of the K6N4-(d) peptide. As a control experiment, when the N-lacking peptide, K6(d), was injected, there were no differences in binding to both A·T and G·C base pairs (Figure 4B). Similarly, the K4N1(d) peptide gave 2-fold higher affinity for A·T than G·C base pairs, but the K4(d) peptide exhibited the same affinity for both A·T and G·C base pairs (panels

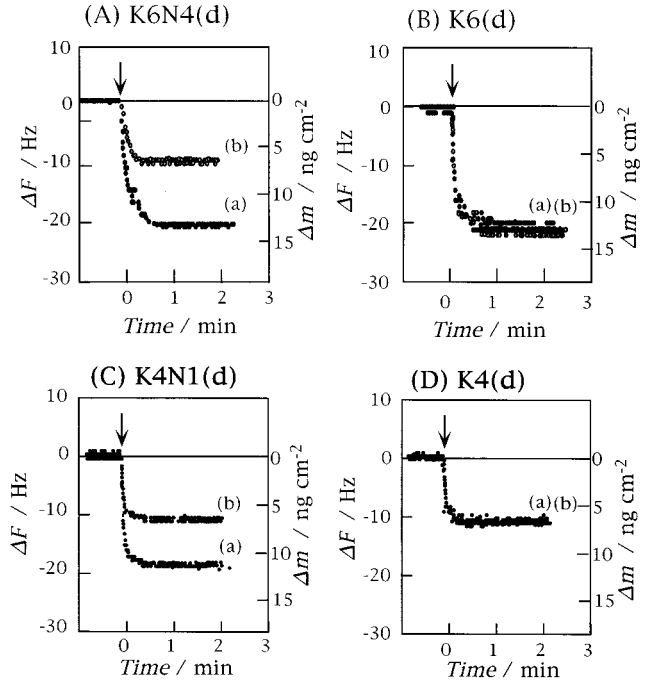

FIGURE 4: Typical time courses of frequency decreases (mass increases) of the **(a)** dA_{30}·dT_{30}- or **(b)** dG_{30}·dC_{30}-immobilized 27 MHz QCM, in response to the addition of **(**A**)** K6N4(d), (B) K6(d), (C) K4N1(d), and **(**D**)** K4(d) peptides [10 °C, pH 7.5, 10 mM phosphate, 40 mM NaCl, [K6N4(d)] = [K6(d)] = 1.0 μM, [K4N1(d)] = [K4d)] = 30 μM, [DNA] on a QCM = 6×10^{-12} mol cm^{-2}].

C and D of Figure 4, respectively). This suggests that one N residue in K4N1(d) leads the selectivity for A·T base pairs, probably due to the hydrogen-bonding interaction between the amide side chain of the N residue and A·T base pairs. Similar AT-selective binding behavior was observed for

Table 1: Maximum Binding Amounts (Δm_{max}) and Binding Constants (K_a) of Oligopeptides for $dA_{30}\cdot dT_{30}$ and $dG_{30}\cdot dC_{30}$ Strands Immobilized on a 27 MHz QCM[a]

peptide	Δm_{max} (ng cm^{-2})		K_a ($\times 10^4$ M^{-1})		K_a ratio	θ_{223} ratio[c]
	A·T	G·C	A·T	G·C	(A·T/G·C)	(A·T/G·C)
K4N4(a)	13 ± 3	15 ± 2	0.85 ± 0.04	1.9 ± 0.3	0.45	
K4(a)			1.8 ± 0.3	2.7 ± 0.3	0.7[b]	
K4N4(c)	25 ± 2	26 ± 2	2.3 ± 0.3	0.6 ± 0.02	3.8	3.1
K4(c)			0.3 ± 0.2	1.9 ± 0.2	1.1[b]	
K4N1(d)	28 ± 2	26 ± 2	2.2 ± 0.3	0.93 ± 0.02	2.4	1.2
K4N4(d)	36 ± 3	29 ± 2	4.4 ± 0.3	2.7 ± 0.2	1.6	2.7
K4(d)			1.2 ± 0.3	1.2 ± 0.3	1.0[b]	
K4N4(e)	28 ± 3	15 ± 2	1.8 ± 1.0	0.90 ± 0.05	2	1.3
K4(e)			0.16 ± 0.04	0.15 ± 0.03	1.1[b]	
K6N4(d)	25 ± 2	24 ± 2	59 ± 5	12 ± 2	5	4.3
K6(d)			11 ± 2	13 ± 2	0.85[b]	

[a] At 10 °C, pH 7.5, 10 mM phosphate buffer, and 40 mM NaCl. [b] From ref *7*. [c] From Figure 7 at 2 μM oligonucleotide.

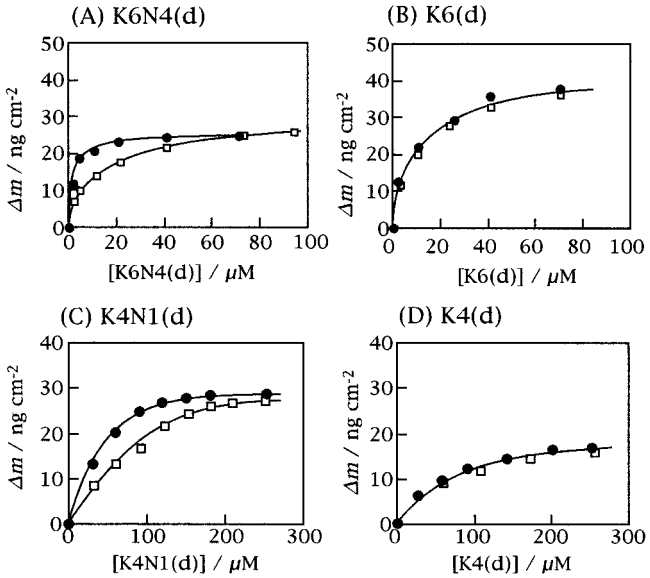

FIGURE 5: Saturation curve fittings for binding amounts of (A) K6N4(d), (B) K6(d), (C) K4N1(d), and (D) K4(d) peptides binding to (●) $dA_{30}\cdot dT_{30}$ or (□) $dG_{30}\cdot dC_{30}$ strands as a function of peptide concentration (10 °C, pH 7.5, 10 mM phosphate, 40 mM NaCl, [DNA] on a QCM = 6×10^{-12} mol cm^{-2}).

K4N4(c) and K4N4(d), and K4N4(e) peptides. On the other hand, the N-lacking peptides, K4(c)−K4(e), exhibited no selectivity.

As control experiments, we confirmed that these peptides hardly bound nonspecifically to the avidin surface without oligonucleotides, and also to the surface of the single-strand oligonucleotide-immobilized avidin surface even at the relatively high peptide concentrations (1−30 μM in the solution).

Maximum Binding Amount (Δm_{max}) and Binding Constant (K_a). Binding amounts (Δm) revealed simple saturation curves as a function of peptide concentrations as shown in Figure 5. These saturation binding behaviors are expressed by eq 1 as a linear reciprocal plot of [peptide]/Δm versus [peptide].

$$\frac{[\text{peptide}]}{\Delta m} = \frac{[\text{peptide}]}{\Delta m_{max}} + \frac{1}{\Delta m_{max} K_a} \qquad (1)$$

Binding constants (K_a) and maximum binding amounts (Δm_{max}) were calculated from the slope and the intercept of eq 1, respectively. The obtained Δm_{max} and K_a values are summarized in Table 1.

CD Spectral Changes. Binding of cationic K-containing peptides to DNA strands could also be confirmed from CD spectral changes in bulk solution (*9b*, *11*, *15*). Since these peptides have four or six positively charged K groups as shown in Figure 2B, they exist in a random coil conformation in the absence of DNA. When these peptides bound to DNA strands, they are expected to form an α-helical conformation resulting from the interaction with phosphate groups. Figure 6 shows typical difference CD spectra indicating the conformation changes of K6N4(d), K4N1(d), and K4N4(c) peptides in the absence and presence of $dA_{30}\cdot dT_{30}$ or $dG_{30}\cdot dC_{30}$ strands in the buffer solution. CD spectra of peptides with DNA strands were subtracted from that of DNA only. In all cases, no precipitation or turbidity was observed. When $dA_{30}\cdot dT_{30}$ strands were added to the K6N4(d), K4N1(d), and K4N4(c) peptide solution, the molecular ellipticity at 223 nm (θ_{223}) increased greatly as a result of the formation of the α-helical peptide structure. On the contrary, CD spectra of these peptides hardly changed in the presence of $dG_{30}\cdot dC_{30}$ strands. The variations of θ_{223} values as a function of added $dA_{30}\cdot dT_{30}$ and $dG_{30}\cdot dC_{30}$ concentrations are shown in panels A and B of Figure 7, respectively. A decrease in the ellipticity at 223 nm means an increase in the α-helical content of peptides. These figures show that only A·T base pairs could promote the α-helical conformation. The ratios of θ_{223} values in the presence of the $dA_{30}\cdot dT_{30}$ or $dG_{30}\cdot dC_{30}$ duplex (2 μM) are summarized in Table 1. The CD spectral changes are in general agreement with the binding selectivity of these peptides for the A·T base pairs.

DISCUSSION

Because 120 ± 3 ng cm^{-2} (~6×10^{-12} mol cm^{-2}) of biotin-$dA_{30}\cdot dT_{30}$ (MW = 18 723) or biotin-$dG_{30}\cdot dC_{30}$ (MW = 18 753) is immobilized on a QCM, a mass increase of 10−12 ng cm^{-2} is expected if one peptide (MW = 1517−1872) binds to one DNA strand. Δm_{max} values of the N-containing peptides are in the range of 13−36 ng cm^{-2} depending on the peptide sequences for A·T base pairs, which are slightly larger than Δm_{max} for G·C base pairs (see Table 1). The K6N4(d) peptide exhibited the largest K_a value (5.9×10^5 M^{-1}) with the highest selectivity (A·T/G·C = 5), which is consistent with the large θ_{223} value in Figures 6A and 7A and Table 1. Since the N-lacking K6(d) peptide

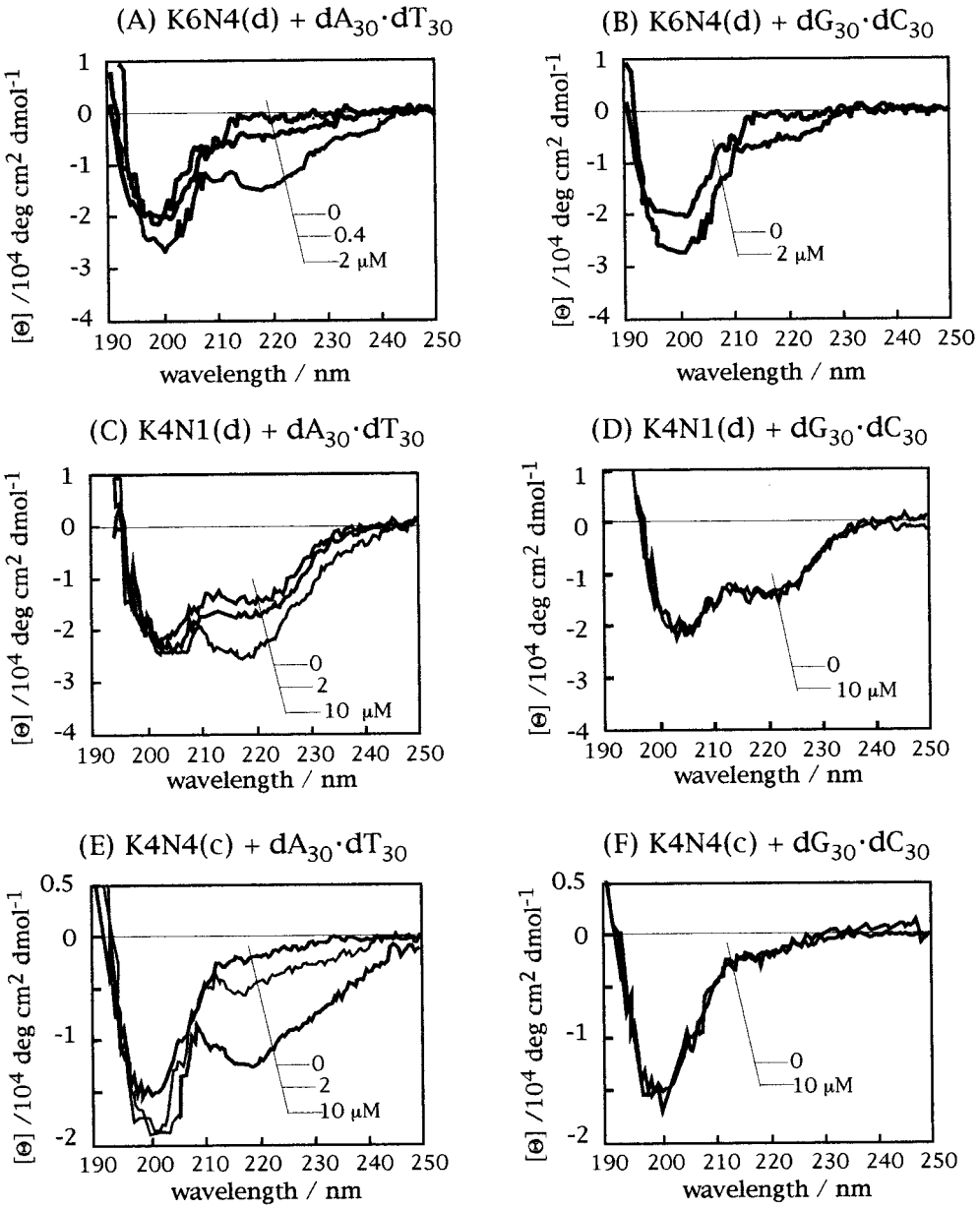

FIGURE 6: Differential CD spectra of peptides as a function of DNA concentration. The spectrum of DNA was subtracted from the spectrum of a mixture of DNA and peptide. Concentrations of added DNAs are given in the figures (10 °C, pH 7.5, 10 mM phosphate, 20 mM NaCl).

exhibited the smaller K_a value with the no selectivity for A·T/G·C strands, it is obvious that the diagonally arranged N residues play an important role in selective binding to the A·T base pairs of the major groove of DNA strands and forming the α-helical structure. The Δm_{max} value (25 ± 2 ng cm^{-2}) of K6N4(d) showed that two peptides bound to one DNA strand.

We have studied the binding of the basic-region leucine-zipper (GCN4-bZIP) motif to the sequence 5′ATGACGTCAT3′ (CRE) duplex, which was immobilized on a 27 MHz QCM through the avidin−biotin linkages in a manner similar to that used in this study (*16b*). The bZIP 56 mer peptides contain both the leucine-zipper region that forms a homodimer of parallel α-helices in the coiled coil region and the two N-terminal basic regions that fit into the major groove of the CRE duplex (see Figure 1A) (*4*). We have also studied the binding behavior of the modified bZIP peptide having only the basic region, in which the two leucine-zipper parts are exchanged with a covalently bonded Cys-Cys linkage (ss-bZIP) (*11*, *16b*). K_a values of bZIP and ss-bZIP peptides for binding to the CRE duplex on the QCM were found to be 3.0 × 10^7 and 1.0 × 10^6 M^{-1}, respectively (20 °C, 20 mM Tris-HCl, pH 7.5, 0.2 M KCl, 2 mM EDTA, 10 mM $MgCl_2$) (*16b*). The 30-fold lower K_a value of ss-bZIP indicates that the leucine-zipper region forming a homodimer plays the important role of putting a DNA strand between two basic regions. That is, the K_a value of ss-bZIP reflects the affinity of the α-helical basic-region peptide for the CRE sequence. The binding constant for binding of the K6N4(d) peptide to the A·T sequence (K_a = 5.9 × 10^5 M^{-1}) is reasonable compared with that for binding of the α-helical ss-bZIP peptide to the CRE sequence (K_a = 1.0 × 10^6 M^{-1}).

K4N4(c), K4N4(d), and K4N4(e) peptides also exhibited relatively high A·T/G·C selectivities (1.6−3.8) with relatively large K_a values, and two peptides are suggested, from Δm_{max} values, to bind per DNA strand. These peptides also

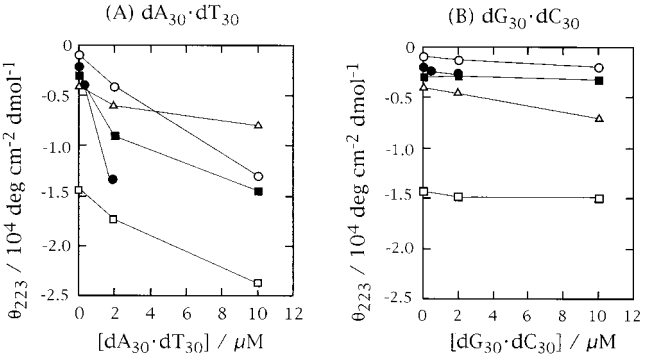

FIGURE 7: Molar ellipticity changes of peptides as a function of the concentration of the (A) dA_{30}·dT_{30} and (B) dG_{30}·dC_{30} duplex in buffer solution: (●) K6N4(d), (□) K4N1(d), (■) K4N4(c), (○) K4N4(d), and (△) K4N4(e) peptides as a function of the concentration of the dA_{30}·dT_{30} and dG_{30}·dC_{30} duplex in buffer solution (10 °C, pH 7.5, 10 mM phosphate, 20 mM NaCl).

exhibited large θ_{223} value changes (Figure 7A). The α-helical conformation of the K6N4(d) and K4N4(c) peptides was largely induced due to the binding to A·T base pairs (panels A and E of Figure 6). On the contrary, K4N1(d) formed the α-helical conformation even in the absence of the DNA strand and the α-helical content was increased in the presence of A·T base pairs (Figure 6C).

The K4N4(a) peptide, having four N residues along the perpendicularly arranged K4 groups, did not show any A·T base pair selectivity (Table 1). From computer-aided CPK molecular models, helical peptides of K6N4(d), K4N4(d), and K4N1(d) were shown to be located in the major groove of the dA30·dT30 strand due to the interaction between cationic K groups of the peptides and anionic DNA phosphates. K4N4(a) exhibited no selectivity, and N residues could not reach the DNA base with concurrent binding of K residues to DNA phosphates.

SUMMARY

On the basis of a well-conserved sequence of natural DNA-binding proteins, we have designed and synthesized DNA binding α-helical peptides with selectivity for A·T base pairs. We found that properly arranged N residues would lead the selectivity for A·T base pairs through specific hydrogen bondings, as shown in the following order: K6N4(d) > K4N4(d) > K4N4(c) > K4N1(d) > K4N4(e). A simplified α-helical model peptide designed from the DNA-binding fragment of proteins can provide useful information about the sequence specificity of proteins. This strategy contributes to the solution of the sequence recognition rules of DNA-binding proteins.

The 27 MHz QCM system yields quantitative detection of in situ binding of small peptide molecules to DNA strands in the aqueous solution without labeling. From frequency changes, binding parameters such as Δm_{max} at the nanogram level and K_a are obtained. It is otherwise difficult to quantitatively detect the amount of small molecules such as oligopeptides bound to DNA strands. The QCM technique should continue to be a useful tool for detection and design of DNA-binding peptides.

ACKNOWLEDGMENT

We gratefully acknowledge Professor H. Mihara for his helpful comments and discussion about peptide syntheses.

REFERENCES

1. (a) Ohlendorf, D. H., Anderson, W. F., Lewis, M., Pabo, C. O., and Matthews, B. W. (1983) *J. Mol. Biol. 169*, 757−769. (b) Ma, P. C. M., Rould, M. A., Weintraub, H., and Pabo, C. O. (1994) *Cell 77*, 451−459. (c) Pabo, C. O., Aggarwal, A. K., Jordan, S. R., Beamer, L. J., Obeysekare, U. R., and Harrison, S. C. (1990) *Science 247*, 1210−1213. (d) Nekludova, L., and Pabo, C. O. (1994) *Proc. Natl. Acad. Sci. U.S.A. 91*, 6948−6952. (e) Pavletich, N. P., and Pabo, C. O. (1991) *Science 252*, 809−817.
2. (a) Bavand, M. R., Wagner, R., and Richmond, T. J. (1993) *Biochemistry 32*, 10543−10552. (b) Schwabe, J. W. R., Chapman, L., Finch, J. T., and Rhodes, D. (1993) *Cell 75*, 567−578.
3. (a) Mondragon, A., Subbiah, S., Almo, S. C., Drottar, M., and Harrison, S. C. (1989) *J. Mol. Biol. 205*, 189−200. (b) Anderson, J. E., Ptashne, M., and Harrison, S. C. (1987) *Nature 326*, 846−852. (c) Aggarwal, A. K., Rodgers, D. W., Drottar, M., Ptashne, M., and Harrison, S. C. (1988) *Science 242*, 899−907. (d) Rodegers, D. W., and Harrison, S. C. (1993) *Structure 1*, 227−240.
4. (a) Konig, P., and Richmond, T. (1993) *J. Mol. Biol. 233*, 139−154. (b) Ellenberger, T. E., Brandl, C. S., Struhl, K., and Harrison, S. C. (1992) *Cell 71*, 1223−1237. (c) Hegde, R. S., Grossman, S. R., Laimins, L. A., and Sigler, P. B. (1992) *Nature 359*, 505−512. (d) Wolberger, C., Vershon, A. K., Liu, B., Johnson, A. D., and Pabo, C. O. (1991) *Cell 67*, 517−528.
5. (a) Suzuki, M. (1993) *EMBO J. 12*, 3221−3226. (b) Suzuki, M., and Yagi, N. (1994) *Proc. Natl. Acad. Sci. U.S.A. 91*, 12357−12361. (c) Suzuki, M. (1989) *J. Mol. Biol. 207*, 61−84. (d) Churchill, M. E. A., and Suzuki, M. (1989) *EMBO J. 8*, 4189−4195. (e) Suzuki, M. (1994) *Structure 2*, 317−326.
6. (a) Helene, C. (1977) *FEBS Lett. 74*, 10−13. (b) Seeman, N. C., Rosenberg, J. M., and Rich, A. (1976) *Proc. Natl. Acad. Sci. U.S.A. 73*, 804−806.
7. Niikura, K., Matsuno, H., and Okahata, Y. (1999) *Chem. Eur. J. 5*, 1609−1616.
8. (a) Walters, L., and Kaiser, E. T. (1985) *J. Am. Chem. Soc. 107*, 6422−6424. (b) Potaman, V. N., and Sinden, R. R. (1998) *Biochemistry 37*, 12952−12961. (c) Dufourcq, J., Neri, W., and Henry-Toulme, N. (1998) *FEBS Lett. 421*, 7−11. (d) Niidome, T., Ohmori, N., Ichinose, A., Wada, A., Mihara, H., Hirayama, T., and Aoyagi, H. (1997) *J. Biol. Chem. 272*, 15307−15312. (e) Wyman, T. B., Nicol, F., Zelphati, O., Scaria, P. V., Plank, C., and Szoka, F. C., Jr. (1997) *Biochemistry 36*, 3008−3017. (f) Zlotnick, A., and Brenner, S. L. (1989) *J. Mol. Biol. 209*, 447−457.
9. (a) Olins, D. E., Olins, A. L., and von Hippel, P. H. (1967) *J. Mol. Biol. 24*, 157−176. (b) Johnson, N. P., Lindstorm, J., Baase, W. A., and von Hippel, P. H. (1994) *Proc. Natl. Acad. Sci. U.S.A. 91*, 4840−4844.
10. (a) Ellenberger, T. E., Brandl, C. J., Struhl, K., and Harrison, S. C. (1992) *Cell 71*, 1223−1237. (b) Strauss-Soukup, J. K., and Maher, L. J. (1997) *Biochemistry 36*, 10026−10032.
11. Morii, T., Yamane, J., Aisawa, Y., Makino, K., and Sugiura, Y. (1996) *J. Am. Chem. Soc. 118*, 10011−10015.
12. (a) Ebara, Y., Itakura, K., and Okahata, Y. (1996) *Langmuir 12*, 5165−5170. (b) Sato, T., Serizawa, T., Ohtake, F., Nakamura, M., Terabayashi, T., Kawanishi, Y., and Okahata, Y. (1998) *Biochim. Biophys. Acta 1380*, 82−92. (c) Ebara, Y., and Okahata, Y. (1994) *J. Am. Chem. Soc. 116*, 11209−11212. (d) Matsuura, K., Ebara, Y., and Okahata, Y. (1996) *Thin Solid Films 273*, 61−65.
13. (a) Marchi-Artzner, V., Lehn, J.-M., and Kunitake, T. (1998) *Langmuir 14*, 6470−6478. (b) Kim, H. J., Kwak, S., Kim, Y. S., Seo, B. I., Kim, E. R., and Lee, H. (1998) *Thin Solid Films 327*, 191−194. (c) Cliffel, D. E., Bard, A. J., and Shinkai, S. (1998) *Anal. Chem. 70*, 4146−4151. (d) Wang, J., Jiang, M., Nilsen, T. W., and Getts, R. C. (1998) *J. Am. Chem. Soc. 120*, 8281−8282. (e) Ijiro, K., Ringsdorf, H., Birch-Hirschfeld, E., Hoffmann, S., Schilken, U., and Strube, M. (1998) *Langmuir 14*, 2796−2800. (f) Ng, S. C., Zhou, X. C., Chen, Z. K., Miao, P., Chan, H. S. O., Li, S. F. Y., and Fu, P. (1998) *Langmuir*

14, 1748−1752. (g) Ward, M. D., and Buttry, D. A. (1990) *Science 249*, 1000−1007.

14. (a) Okahata, Y., Ebato, H., and Taguchi, K. (1998) *J. Chem. Soc., Chem. Commun.* 1363−1365. (b) Okahata, Y., Kimura, K., and Ariga, K. (1989) *J. Am. Chem. Soc. 111*, 9190−9194. (c) Okahata, Y., and Ebato, H. (1991) *J. Chem. Soc., Perkin Trans. 2*, 457−479.
15. Padmanabhan, S., Zhang, W., Capp, M. W., Anderson, C. F., and Record, M. T., Jr. (1997) *Biochemistry 36*, 5193−5206.
16. (a) Niikura, K., Matsuno, H., and Okahata, Y. (1998) *J. Am. Chem. Soc. 120*, 8537−8538. (b) Okahata, Y., Niikura, K., Sugiura, Y., Sawada, M., and Morii, T. (1998) *Biochemistry 37*, 5666−5672. (c) Okahata, Y., Kawase, M., Niikura, K., Ohtake, F., Furusawa, H., and Ebara, Y. (1998) *Anal. Chem. 70*, 1288−1296. (d) Caruso, F., Rodda, E., Furlong, D. N., Niikura, K., and Okahata, Y. (1997) *Anal. Chem. 69*, 2043−2049.
17. Talanion, R. V., McKnight, C. J., and Kim, P. S. (1990) *Science 249*, 769−771.

BI001699O